

# Numerical and Experimental Investigation of Mixed-Mode Fracture of Cement Paste and Interface under Three-Point Bending Test

S. Al Dandachli, F. Perales, Y. Monerie, F. Jamin, M. S. El Youssoufi, C. Pelissou

**Abstract**—The goal of this research is to study the fracture process and mechanical behavior of concrete under I–II mixed-mode stress, which is essential for ensuring the safety of concrete structures. For this purpose, two-dimensional simulations of three-point bending tests under variable load and geometry on notched cement paste samples of composite samples (cement paste/siliceous aggregate) are modeled by employing Cohesive Zone Models (CZMs). As a result of experimental validation of these tests, the CZM model demonstrates its capacity to predict fracture propagation at the local scale.

**Keywords**—Concrete, cohesive zone model, microstructure, fracture, three-point flexural test bending.

## I. INTRODUCTION

CONCRETE is a quasi-brittle material with a high degree of heterogeneity. The presence of multiple phases in concrete (cement paste, sand, gravel, porosity, etc.) leads in a gradient of mechanical characteristics, notably around the aggregates, where an Interfacial Transition Zone (ITZ) is formed. This disparity in microstructure characteristics has a significant impact on the process of damage and cracking, making fracture propagation in concrete difficult to predict.

The experimental results reveal that cracks can occur at the interfaces of relatively heterogeneous materials like concrete due to debonding and subsequently spread through the cement paste or mortar, or vice versa [9]. These observations highlight the significance of conducting a local numerical investigation of crack propagation at the level of pure cement paste and at the interface between the cement paste and the aggregate. Analyzing the phenomena of local crack propagation, two mechanisms are commonly distinguished: the emergence of a damaged zone at the crack tip and the occurrence of the crack. These mechanisms result in two numerical behaviors: (i) linear in the absence of cracking in the material; and (ii) nonlinear, related to the appearance of microcracks and damage or steady growth of cracks. The CMZ is one of the modeling methodologies used here for fracture mechanisms in heterogeneous materials. This model allows us to define the fracture as a displacement jump between cohesive elements. CZM model will be used to execute a numerical study of fracture propagation at the local scale of cementitious material.

The simulations will be compared to experimental applications in accordance with the program outlined in Section II.

Sirine Al Dandachli is with University of Montpellier, France (e-mail: dandachlicirine@gmail.com).

## II. SPECIMEN PREPARATION AND EXPERIMENTAL SET-UP

### A. Samples

The studies in this paper are performed on two types of parallelepiped samples (dimensions: 10 x 10 x 30 mm): a specimen of cement paste notched at a 60° angle, and a composite made of cement paste attached to a silica-type aggregate (quartz) whose interface angle ranges between 30° and 90° (see Fig. 1). The notch on the cement paste sample allows for the location of the crack's initiation. On composite specimens, a notch is not required because the contact with the aggregate is sufficient to locate the fracture (interfacial failure).

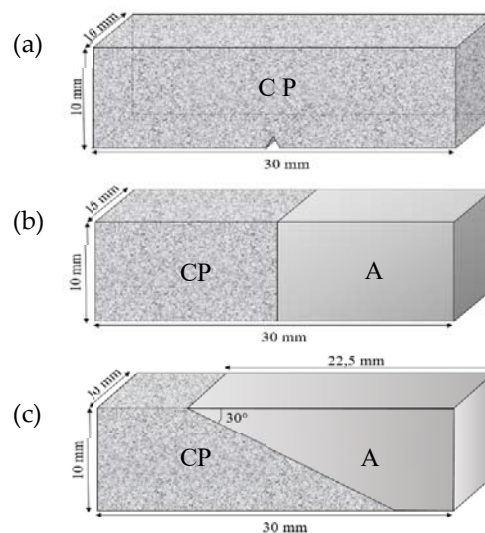


Fig. 1 Specimens' geometric descriptions: (a) cement paste; (b) straight aggregate composite with a 90° interface angle and (c) 30° inclined aggregate composite (CP: Cement Paste and A: Aggregate)

TABLE I  
MATERIAL PROPERTIES

Aggregate	Mineralogical nature
	Quartz (98% SiO <sub>2</sub> )
Cement Paste	
Cement class	CEM I 52,5 R CE CP2 NF
Water-to-Cement ratio	0,47

The materials used to create the test specimens are listed in Tables I and II. Silicone molds are used to make these specimens. After preparation, the samples are removed from the

molds after 24 hours and conditioned in lime-saturated water for 40 days before being tested.

TABLE II  
 MINERALOGICAL AND CHEMICAL COMPOSITIONS OF CEMENT

Components	Content (%)
C <sub>3</sub> A	11
C <sub>4</sub> AF	8
C <sub>2</sub> S	66
C <sub>3</sub> S	10

### B. Experimental Set-Up

Concrete behavior at the local scale necessitates investigation under complex loading conditions. To answer this need, an adaptable three-point bending test bench (see Fig. 2) was designed to allow for adjustment in loading conditions and specimen geometries.

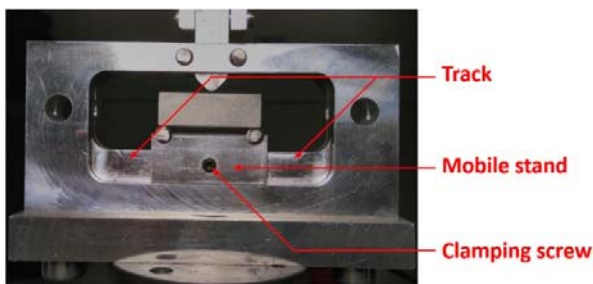


Fig. 2 Design of the modular three-point flexion bench [1]

The distance between the point of load application and the center of the sample is referred to as the eccentricity  $dx$  in the following. For notched cement paste specimens, four loading positions with  $dx$  equal to 0 cm (centered loading), 2.5, 5, and 7.5 mm are tested experimentally. The composite specimens are tested on the same bending bench with centered loading ( $dx = 0$ ), but with a difference in specimen configuration: in the first configuration (denoted C1), the loading is applied to the silica aggregate and, in the second (denoted C2), it is applied to the cement paste (see Fig. 3).

The specimen is positioned on the bending bench with the patterned side facing a high-resolution camera "acA5472-17um - Basler ace" mounted on a fixed gantry. Through precision control of the "MTS" compression machine, a loading speed of 10  $\mu\text{m/s}$  is applied. After post-processing the findings with CIN digital image correlation software, the displacement field can be experimentally seen, from which the fracture propagation path within the specimens can be determined in both cases. The experimental results will be compared to the numerical results reported in the following sections.

## III. MODELING

### A. Numerical Model: Cohesive Zone Model - CZM

The Cohesive-Volumetric Finite Element (CVFE) approach involves "collapsing" the finite element mesh and taking into account the decohesion of the interfaces of its volumic elements. A so-called "cohesive" law links the finite components trying to describe the traction separation

phenomena of the interface. In general, these cohesive laws connect the stress on the height of the crack lips to its displacement discontinuity. The cohesive zone at the interface is represented by two damageable "springs" with two stiffnesses (denoted  $C_N$  and  $C_T$ ), allowing the description of two failure modes: normal and tangential (see Fig. 4).

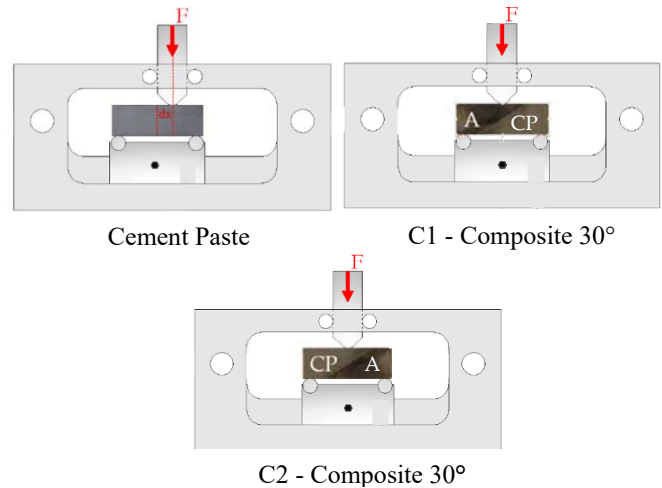


Fig. 3 Geometry and boundary conditioned of samples subjected to three-point bending test (CP: Cement Paste and A: Aggregate)

The "XPER" software [2], [3] developed at Institute of Radioprotection and Nuclear Safety (IRSN) within the framework of the joint MIST laboratory (joint laboratory IRSN/CNRS/University of Montpellier) is the numerical tool employed. For numerical simulations of cementitious materials, the cohesive law, known as MAL in XPER, was used [2], [3]. This cohesive law is determined by three parameters:  $\sigma_i$  (critical cohesive stress),  $w_i$  (cohesive energy), and  $C_i$  (initial cohesive stiffness) for each normal mode ( $i = 1$ ) and tangent mode ( $i = 2$ ) (see Fig. 5).

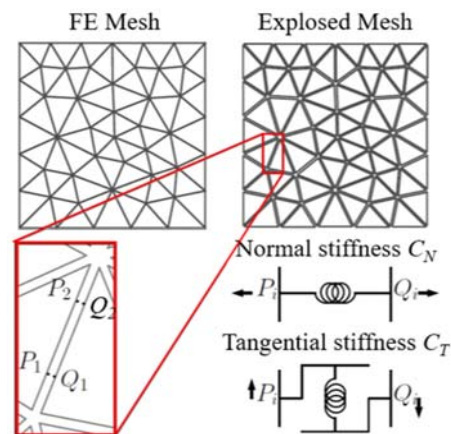


Fig. 4 Illustration of the concept of the Volumic-Cohesive Finite Element Approach [4]

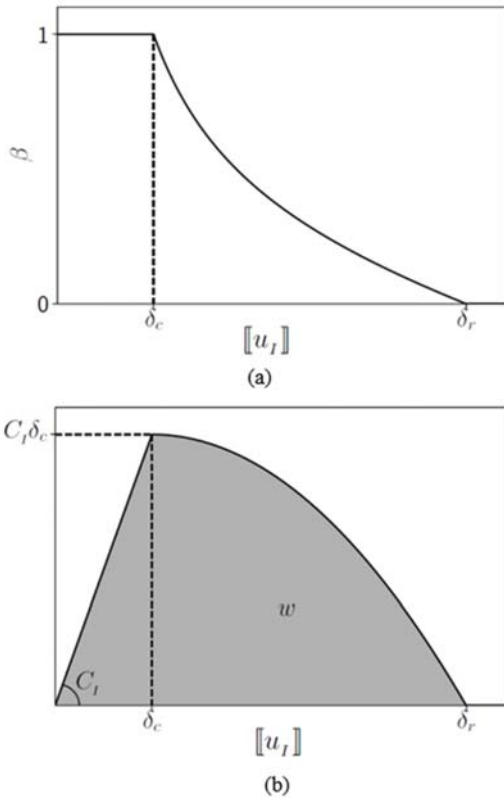


Fig. 5 The form of cohesive law applied: (a) Evolution of the damage according to the normal/tangent displacement discontinuity; (b) Cohesive stress associated with a normal/tangent displacement jump [5]

A damage occurs between the elements after a critical displacement ( $\delta_c$ ) ( $\llbracket u \rrbracket > \delta_c$ ) jump, regardless of the loading mixity (the same one in normal and tangent modes). Furthermore, the critical cohesive stresses of the normal and tangential modes may be given by:

$$\sigma_N^{max} = C_N \delta_c = \left( \frac{1}{2} + \frac{C_N}{2C_T} \right) \sigma^{max} \quad (1)$$

$$\sigma_T^{max} = C_T \delta_c = \left( \frac{1}{2} + \frac{C_T}{2C_N} \right) \sigma^{max} \quad (2)$$

and the cohesive fracture energy is by:

$$w_N = \left( \frac{1}{2} + \frac{C_N}{2C_T} \right) w \quad (3)$$

$$w_T = \left( \frac{1}{2} + \frac{C_T}{2C_N} \right) w \quad (4)$$

It is important to note that the ratios of the normal and tangential cohesive stresses, as well as the cohesive energies, are identical.

### B. Finite Element Meshes

For the two specimens, a uniform mesh of the Delaunay type with a characteristic size  $l_{mesh} = 0.2$  mm (see Fig. 6) is generated in GMSH. Based on the calculations conducted during Delaume's research [4], a time step of  $10^{-8}$  s is retained

for the simulations. The vertical loading is delivered at a speed of  $10 \mu\text{m/s}$  [5]. A volumic law is adopted between all of the mesh's elements. Thus, a cohesive zone law is described for all interfaces: cement paste/cement paste, cement paste/aggregate and aggregate/aggregate.

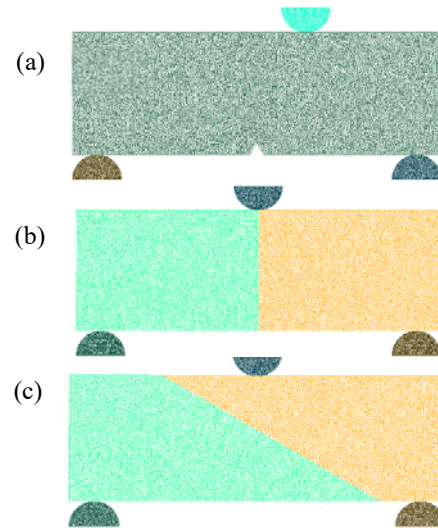


Fig. 6 The mesh for: (a) Eccentric three-point bending; (b) Composite with straight aggregate ( $90^\circ$ ); (c) Composite with aggregate slanted at  $30^\circ$

The initial cohesive stiffnesses  $C_N$  and  $C_T$  for the three-point bending test on the notched cement pastes were determined using Blal's practical criterion [6] to limit the dependency of mechanical response (force/displacement) on the characteristic size of the mesh. The cohesive parameters for different phases are shown in Table III. A ratio of 10 between normal and tangential values is proposed [7].

TABLE III  
ELASTIC AND COHESIVE PROPERTIES OF THE DIFFERENT MATERIALS

Parameters	Aggregate	Cement paste	Interface
$C_N$ [MPa/m]	$1.21 \times 10^{13}$	$7.7 \times 10^{11}$	$6.7 \times 10^{11}$
$C_T$ [MPa/m]	$5.1 \times 10^{13}$	$9.8 \times 10^{11}$	$8.8 \times 10^{11}$
$\sigma_N$ [MPa]	$6 \times 10^2$	3.1	0.4
$\sigma_T$ [MPa]	$1.2 \times 10^3$	6.2	1.2
$w_N$ [J/m <sup>2</sup> ]	$10^5$	25	2.5
$w_T$ [J/m <sup>2</sup> ]	$10^6$	250	25
Young modulus E [MPa]	$65 \times 10^3$	$15 \times 10^3$	-
Poisson's ratio $\nu$	0.22	0.2	-

### Numerical Results

#### 1) Cement Paste: Non-Symmetrical Three-Point Bending Tests

First, the results of simulations performed on cement paste specimens with load eccentricities of 0, 2.5, 4, 5, 6, and 7.5 mm are presented. Fig. 7 shows a visualization of displacement fields.

In mode I, a crack propagates from the notch (concentrated load) throughout the center of the specimen when  $dx = 0$  mm. The propagation is in mixed mode for  $dx = 2.5, 4$  and  $5$  mm, and further fracture begins also in notch and reaches the place

of application of the load. However, at an eccentricity of 2.5 mm, the crack first propagates in normal mode or mode I, then branched out in the cement paste to join the loading point application, which was not the case for  $dx = 4$  and 5 mm, where the crack propagates in mixed mode from its initiation.

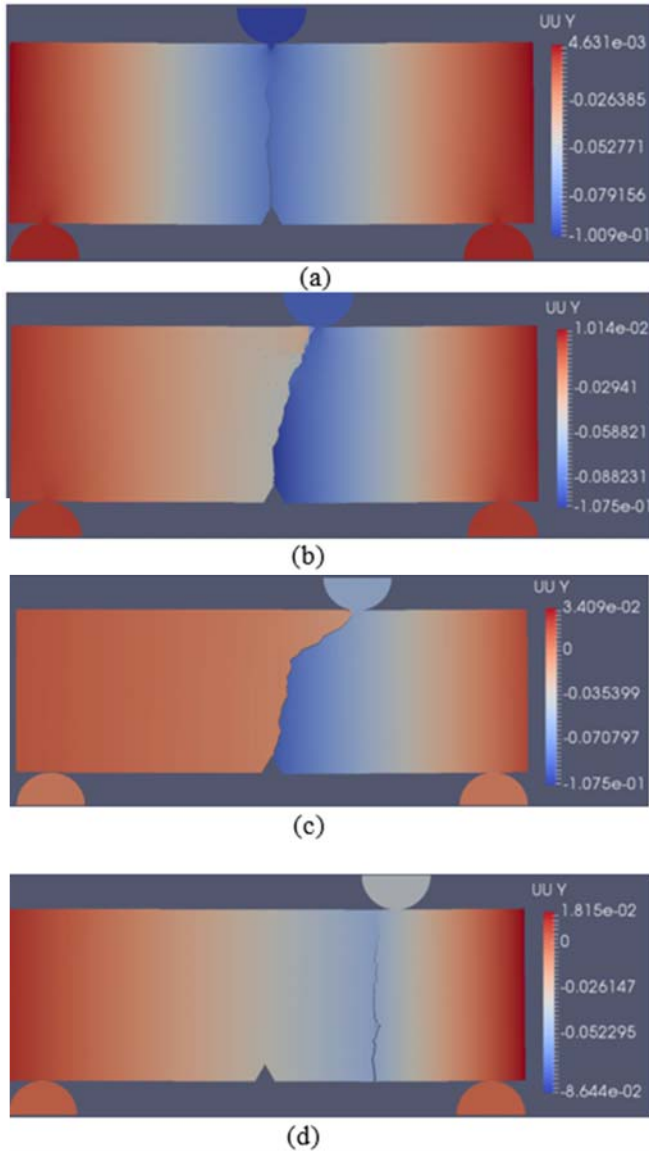


Fig. 7 Displacement fields of cement paste specimens in three point flexural test with an eccentric load of  $dx$

In the cases of eccentricity of 6 mm and 7.5 mm, however, the fracture does not initiate from the notch, but rather from the bottom edge of the specimen on the same horizontal side as the point load application.

The curves in Fig. 8 quantify these results. It is clear that the more the specimen is stressed in mixed mode, the stiffer the structure become, as does its resistance to rupture. A research by Jenq [8] within the context of the investigation of the mixed pattern of crack propagation during a three point bending on concrete prisms by displacing the notch with regard to the centered loading supports our results.

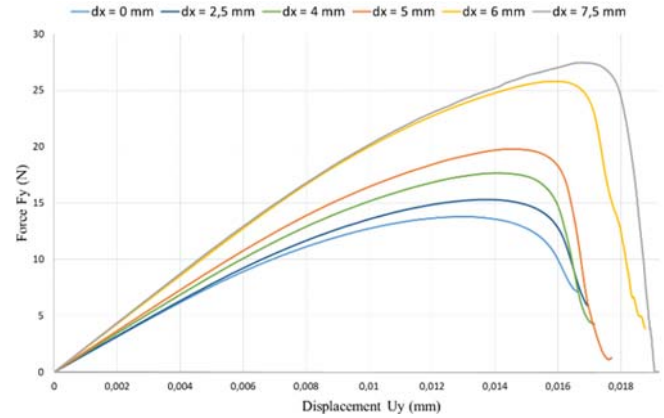


Fig. 8 Mechanical behaviors of cement paste specimens under non-symmetrical three-point bending tests

### 2) Three-Point Bending Tests with Centered Load on a Composite with an Oblique Interface

Two composite specimen configurations, C1 and C2, are studied. For each configuration, three inclinations of the cement paste/aggregate interface ( $30^\circ$ ,  $45^\circ$ , and  $60^\circ$ ) are considered in addition to a composite with a straight interface. Fig. 9 represents the displacement fields and fracture propagation in these simulations.

The fracture propagates along the interface in both configurations C1 and C2 (the weakest phase). However, when the load is applied to the cement paste in the C2 configuration, the fracture spreading in the interface deviates in the cement paste towards the loading point.

The curves in Fig. 10 indicate that as the interface is loaded in mixed mode by raising the inclination of the aggregate, the specimen's resistance and fracture energy increase. As a result, specimens from C1 configuration, where the load is applied to the silica aggregate, resist more than those from C2 configuration. This response is reasonably common due to the hardness of the contact point, as silica is more rigid than cement paste.

## IV. COMPARISON BETWEEN EXPERIMENTAL AND NUMERICAL RESULTS

The tests were carried out experimentally on the two specimen types, due to the setup described in the preceding section. On notched cement paste specimens, four loading locations with eccentricities  $dx$  equal to 0 mm (centered loading); 2.5 mm; 5 mm; and 7.5 mm are investigated on 10 samples each. Three composite specimen forms are evaluated (6 samples per configuration) for the composite specimens: straight interface ( $90^\circ$ ); inclined interface at  $30^\circ$ ; and inclined interface at  $60^\circ$  where the loading is centered ( $dx = 0$ ). Figs. 11 and 12 show the experimental results of these tests, which are compared to a numerical simulation of a corresponding test.

The fracture propagates similarly experimentally and computationally in the eccentric three-point bending tests on cement paste (see Fig. 11), where the fracture generally initiates at the notch and propagates in the cement paste in mode I when  $dx = 0$  mm or in mixed mode in other circumstances.

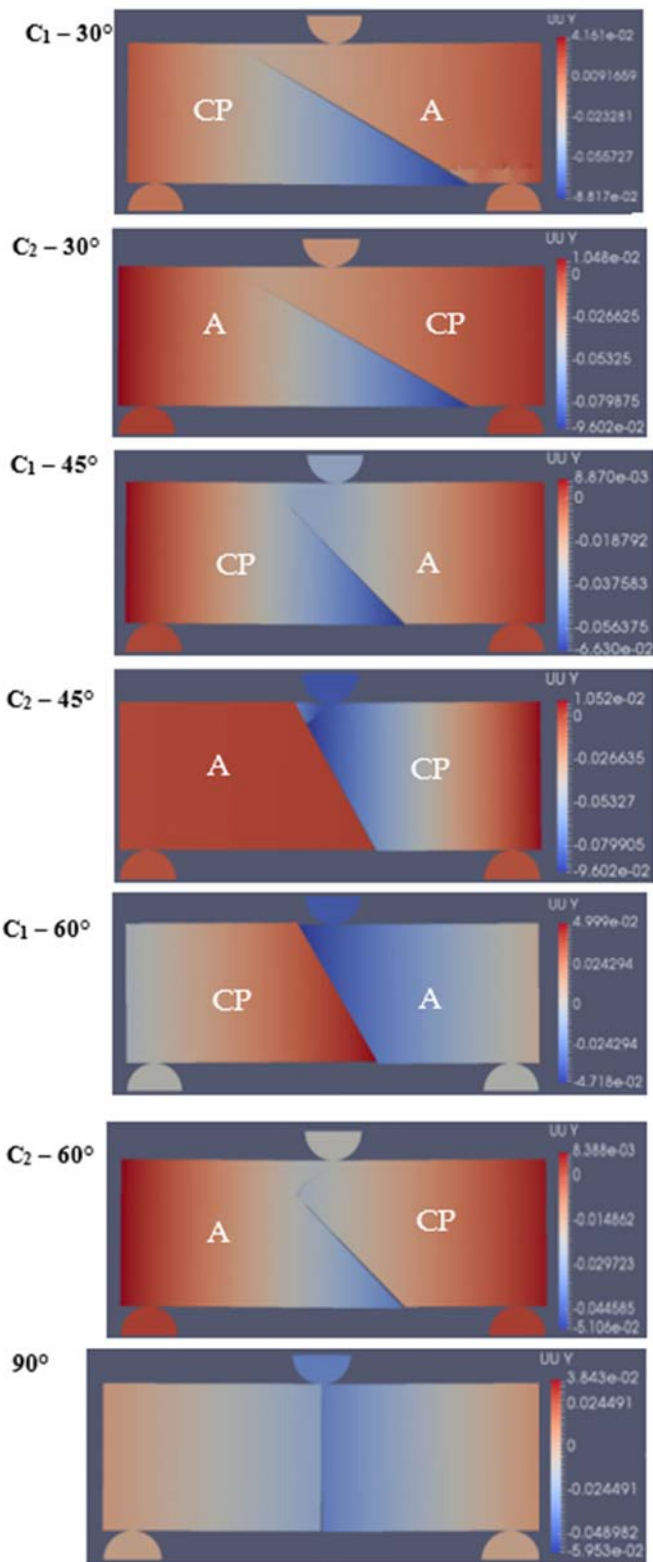


Fig. 9 Displacement fields of composite specimens subjected to three-point bending with centered load with inclined aggregate (30°, 45°, and 60°) and straight aggregate in two configurations (C1 and C2)

For the composite test results, the crack begins and propagates in the cement paste, then bifurcates to propagate in

the interface in the C1 configuration. In the case of C2 configuration, the fracture propagates mostly in the interface and the cement paste after beginning on the tensile face at the matrix-aggregate connection.

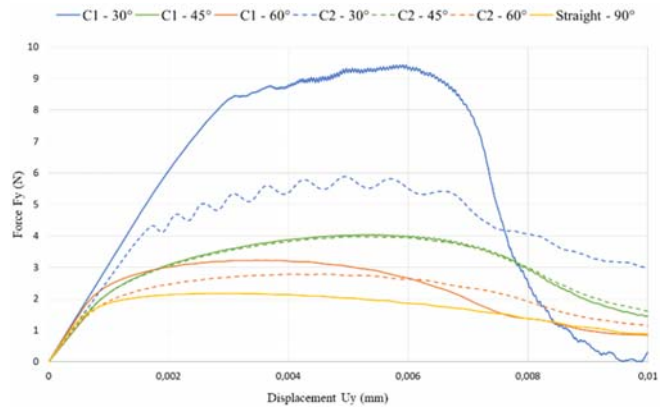


Fig. 10 Mechanical behaviors of composite specimens under symmetrical three-point bending tests

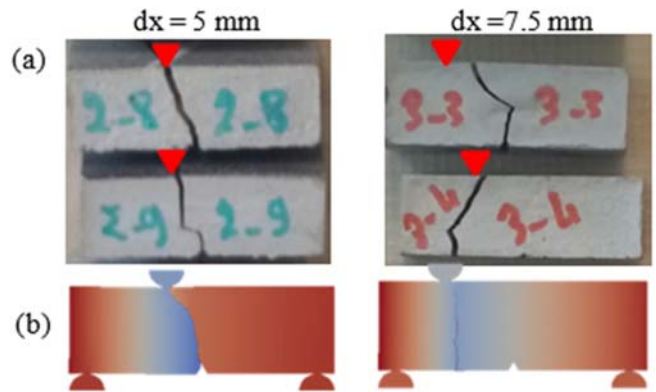


Fig. 11 Results of cement paste specimens under three-point bending with an eccentric load of dx: (a) experimentally (rupture profiles) and (b) numerically (rupture profiles and displacement fields)

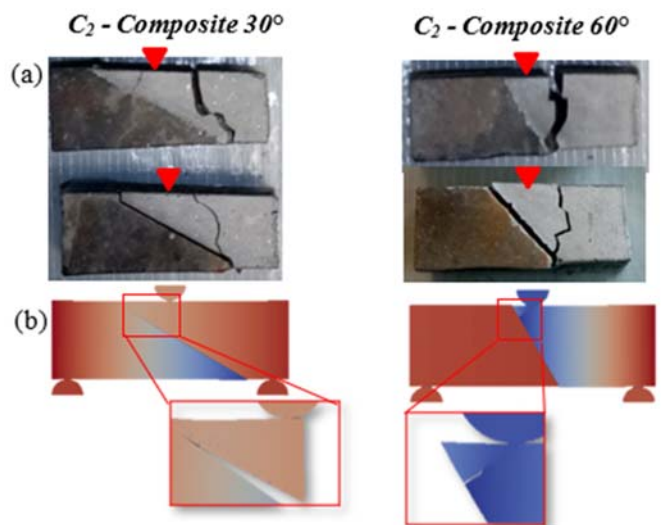


Fig. 12 Results of composite specimens under three-point bending with a centered load: (a) experimentally (rupture profiles) and (b) numerically (rupture profiles and displacement fields)

## V. CONCLUSION

This paper summarizes local-scale simulations of the mechanical behavior of cement paste and of the cement paste/aggregate interface under loading in normal mode and in mixed mode by a three-point bending device adapted for each specimen. The modeling of the cracking at the level of the cementitious matrix and the interface is carried out based on the model of the cohesive zones. A cohesive law is introduced on all mesh interfaces for the two phases: cement paste and interface (cement paste/aggregate).

The simulations match the present experimental results. Therefore, the numerical findings demonstrate that when the mixing ratio is high, the fracture energy and material resistance are significant for the two sample types: cement paste and composite. However, despite the similarity of experimental and numerical responses in terms of crack path, the experimental results do not match to those acquired numerically. Experimentally, the cement paste and the interface have fragile behavior, while a ductile behavior is numerically obtained.

The experimental results need to be compared to numerical simulations in order to calibrate and estimate the cohesive parameters of the numerical model based on the mechanical response.

## REFERENCES

- [1] A. Gîrboveanu, "Approche multi-échelle de la dégradation chimique de matériaux cimentaires Application à la durabilité des ouvrages en béton" *Thesis, University of Montpellier*, 2020.
- [2] F. Perales, S. Bourgeois, A. Chrysochoos, and Y. Monerie, "Two field multibody method for periodic homogenization in fracture mechanics of nonlinear heterogeneous materials". *Engineering Fracture Mechanics*, 75(11), pp.3378-3398, 2008.
- [3] F. Perales, F. Dubois, Y. Monerie, B. Piar, & L. Stainier, "A nonsmooth contact dynamics-based multi-domain solver: code coupling (xper) and application to fracture". *European Journal of Computational Mechanics*, 19(4), 389-417, 2010.
- [4] E. Delaume, L. Daridon, F. Dubois, Y. Monerie, & F. Perales, "Méthode de raffinement local adaptatif multi-niveaux pour la fissuration des matériaux hétérogènes", in *13e colloque national en calcul des structures*, May 2017.
- [5] J. Lhonneur, "Approche par changement d'échelle du vieillissement des bétons: expérimentations et simulations numériques" *Thesis, University of Montpellier*, 2021.
- [6] N. Blal, L. Daridon, Y. Monerie, & S. Pagano, "Micromechanical-based criteria for the calibration of cohesive zone parameters". *Journal of computational and applied mathematics*, 246, 206-214, 2013.
- [7] A. Socie, F. Dubois, Y. Monerie, & F. Perales, "Multibody approach for reactive transport modeling in discontinuous-heterogeneous porous media". *Computational Geosciences*, 25(5), 1473-1491, 2021.
- [8] Y. S. Jenq, & S. P. Shah, "Mixed-mode fracture of concrete". *International Journal of Fracture*, 38(2), 123-142, 1988.
- [9] Ł. Skarżyński & J. Tejchman "Experimental Investigations of Fracture Process in Concrete by Means of X-ray Micro-computed Tomography". *International Journal for Experimental Mechanics*, 52, 26-45, 2016.

**Sirine Al Dandachli** was born in Machta Hammoud, Lebanon, on April 19, 1997. She is currently pursuing a doctoral degree through a collaboration between the CNRS, the University of Montpellier (UM), and the Institute for Radiation Protection and Nuclear Safety (IRSN). At this point, the thesis is in its third year. She was accepted to do her fifth year of study (2020) in a double degree with the École Normale Supérieure of the University of Paris Saclay, where she obtained two diplomas at the end of this year (2019-2020): Diploma in Civil Engineering (structure specialty) and Master 2 in Research in Materials and Structures in Civil Engineering from the University of Paris Saclay.

In semester 1 of her research master's program, she conducted an academic internship at the laboratory of mechanics and technology in Cachan (LMT), France, titled "Reversible Order-Disorder Transition in Ettringite-Metaettringite Conversion." She completed a research internship at the Energies and Atomic Energy Commission CEA, Paris, on Study of the "Damage to Concrete Structures under Creep and Drying". His thesis work has recently enabled him to attend three national conferences: CSMA 2022, CFM 2022, and NoMad 2022, as well as submit two articles. Here are two articles and one conference from marter 2:

- i. Honorio, T., Maaroufi, M., Al Dandachli, S. & Bourdot, A., 2021. Ettringite hysteresis under sorption from molecular simulations. *Cement and Concrete Research*, 150, p.106587.
- ii. Tsitova, A., Bernachy-Barbe, F., Bary, B., Al Dandachli, S., Bourcier, C., Smaniotto, B., & Hild, F. (2022). Damage Quantification via Digital Volume Correlation with Heterogeneous Mechanical Regularization: Application to an In Situ Meso-Flexural Test on Mortar. *Experimental Mechanics*, 62(2), 333-349.
- iii. Honorio, T., Al Dandachli, S., & Bourdot, A. (2021, January). Reversible order-disorder transition in ettringite-metaettringite conversion. In *Conference: 14th World Congress on Computational Mechanics (WCCM) & ECCOMAS Congress (2020)*.